Kinetic Models of Oxygen Thermochemistry Based on Quasi-Classical Trajectory Analysis

Daniil A. Andrienko* and Iain D. Boyd†

University of Michigan, Ann Arbor, Michigan 48109

Recent progress in state-resolved kinetic models of thermal relaxation and dissociation of oxygen based on high-fidelity transition rate coefficients is presented. Specifically, three types of collisions encountered in high-temperature flows are discussed: O_2–O, O_2–N, and O_2–N_2. For these molecular systems, the thermal relaxation times and dissociation rate coefficients, obtained from extensive trajectory simulations, are compared with existing experimental data. A new set of calculations for O_2–N_2 on an ab-initio potential energy surface is presented. Accuracy of multitemperature models is assessed based on comparison with the solution of master equations. Recommendations for adjustable parameters employed in multitemperature models are provided.

I. Introduction

RECENT progress in hypersonic aerothermochemistry is associated with the modeling of nonequilibrium relaxation and dissociation from first principles using quantum-mechanical and semi- and quasi-classical methods. The initial capacity for such research was formed by the ever-increasing computational power that made statistical methods tractable, as well as by the variety of potential energy surfaces (PESs), developed for studies of low-temperature kinetics in the upper atmosphere [1–3].

Although a large amount of previous work regarding the nonequilibrium processes in high-temperature gases have concentrated on the state-resolved chemistry of nitrogen [4–11] and nitric oxide [12] due to the importance of these species in reentry and combustion problems, thermochemistry of oxygen has received little attention. This is because the atmosphere contains only one-fifth molar fraction of oxygen, and it dissociates easily under harsh reentry conditions. However, historical success and setbacks of hypersonic programs [13] have directed research in the study of oxygen nonequilibrium thermalization at lower speeds that correspond to the flight conditions of airbreathing hypersonic vehicles.

For diatomic oxygen, the most important collisions in terms of rovibrational relaxation and dissociation are observed with molecular oxygen and nitrogen as well as with atomic oxygen. Currently, only the latter type of collisions is studied in detail. For the O_2–O system, a number of PESs [14–17] of different fidelity are available due to the important property of the O_3 molecule to absorb harmful ultraviolet radiation [18]. The open-shell electrons of oxygen greatly complicate the treatment of ozone with standard methods. Such problems include nonadiabatic coupling between 27 PESs of the ground state of ozone, presence of reef structure that causes negative temperature dependence of rate coefficients, and isotope effect [1]. High-temperature kinetics of O_2–O collisions received special attention recently due to anomalously high rate coefficients (RCs) of vibrational transitions [19–23]. This phenomenon is associated with the small potential barrier in the entrance/exit channel of the O_2–O interaction. This subject is discussed in detail in the following sections.

The study of collisions of molecular oxygen with other diatomic air species is limited to low temperatures (say, 1000 K). There are a number of O_2–O_2 [3,24,25] and O_2–N_2 [2,26] PESs; however, they are designed only for low-energy collisions. In many cases, these PESs are either limited to a rigid rotor approximation, use empirical data to approximate the intermolecular forces, or do not describe the potential energy in bond-breaking collisions. Nevertheless, the semi- and quasi-classical calculations, conducted on these PESs, showed good agreement with measurements in the rates of vibration–translation (VT) and vibration–vibration (VV) energy transfer between diatomic species at room temperatures [27]. The interest in such kinetic models is dictated by the disagreement in theoretical and experimental predictions of ozone formation rates [1], probably due to some shadow mechanisms involving vibrationally excited O_2 [28,29].

Only recently the investigation of bimolecular collisions at higher temperatures received special attention [30,31] due to the availability of ab-initio four-body PESs. Six-dimensional N_4 PESs based on accurate quantum calculations were developed in the NASA Ames Research Center [32] and in the University of Minnesota [33]. More interesting, in the context of the present paper, is the recent global O_2N_2 PES by Varga et al. [31]. However, sampling all rovibrational states with good statistical accuracy using quasi-classical trajectory (QCT) simulations appears to be computationally intractable using these high-quality PESs. One of the possible ways to overcome this difficulty is the direct molecular simulation method, developed by Koura [34]. Although this approach makes it possible to obtain the average macroscopic parameters, such as vibrational and rotational relaxation times and the quasi-steady-state (QSS) dissociation RC of thermally and chemically nonequilibrium gas mixtures, this method does not allow extraction of the state-specific transition RCs that are typically required for detailed kinetic modeling and interpretation of experiments.

The present paper features the QCT calculations, conducted on the new O_2N_2 PES, and compares the global dissociation RCs and vibrational relaxation time with existing experimental data. The VT and VV energy transfer RCs for selected states are compared with other semiclassical calculations as well. The limitations and applicability of the present technique is discussed. The previous studies of O_2–O and O_2–N molecular systems are revisited and summarized, and general remarks about the computational cost of these three molecular systems are given. In Sec. II, the state-specific and multitemperature models are discussed. Section III presents the discussion of O_2–O, O_2–N, and O_2–N_2 molecular systems. Conclusions are drawn in Sec. IV.

II. Computational Approach

Molecular dynamics approaches can be tentatively divided into quantum [35–37], semiclassical [38–41], and quasi-classical [42,43] methods. The applicability of these methods is defined by the needs

*Postdoctoral Research Fellow, Department of Aerospace Engineering, 1320 Beal Avenue.

†James E. Knott Professor, Department of Aerospace Engineering, 1320 Beal Avenue.

of a particular problem, such as necessity in the exact quantization of a product's final state, accurate treatment of interference effects, importance of multidimensional tunneling effects, and so on. Without providing further discussion on this matter, one should note that there are only a few alternatives to the QCT method when attempting to resolve all possible rovibrational state-specific cross sections at high kinetic energies with sufficient statistical accuracy. On the other hand, it is worth mentioning that the QCT method fails to provide accurate results at some conditions [42]. This occurs due to quantum effects, such as tunneling and complex phase accumulation [42]. Recently, a significant difference in O_2–Ar vibrational relaxation times, obtained via quasi-classical and quantum methods was demonstrated at temperatures below 3000 K [44]. In the present work, O_2–N_2 RCs, obtained via the QCT, are compared with semiclassical calculations [45]. These results indicate that the quasi-classical propagation of trajectories for these species should be treated with caution as well.

The QCT method for three (atom–diatom) and six (diatom–diatom) degrees of freedom yields 12 and 18 Hamiltonian equations, when recognized that the center of mass is a cyclic coordinate and the momentum conjugate to that coordinate is a constant of motion. These numbers can be reduced to 8 and 14 by applying the conservation law of total energy and total angular momentum. However, this would considerably complicate the mathematical formulation of the governing equations. On the contrary, the semiclassical (SC) coupled approach, proposed by Billing [38], involves additional time-dependent Schrödinger equations, for which the number is proportional to the number vibrational states involved in a trajectory simulation. At hypersonic temperatures, when the population of all vibrational states must be captured, such a method becomes computationally intractable.

Details of the QCT method, adopted in the present work, are given elsewhere [20,44]. In summary, each trajectory is initialized by explicit assignment of initial vibrational and rotational quantum numbers and collision energy. This was done to allow for a flexible analysis of state-specific transitions during subsequent kinetic modeling. Other variables, such as impact parameter, orientation angles, and vibrational phase, are sampled randomly. The number of trajectories in each batch varies between 1000 and 10,000. The statistical uncertainty of most RCs is less than 15%.

Table 1 presents a summary on available databases of state-resolved O_2 chemistry [46,47]. These databases have been generated using the QCT method on PESs of different fidelity. For all three atom–molecule systems, listed in Table 1, the computational time reflects the amount of resources required to resolve the cross-sectional data for all possible precollisional rovibrational states. In the case of O_2–N_2, such calculations are intractable. Instead, simulations are performed for 160 pairs of initial vibrational states of oxygen and nitrogen with the initial rotational state sampled according to the Boltzmann distribution at $T_r = 10{,}000$ K. The number of trajectories reflects the size of database for each pair of species.

The O_2–Ar system employs the pairwise analytical PES. These calculations have demonstrated sufficient accuracy due to the closed-shell electronic configuration of the projectile species. The simulations of O_2–O and O_2–N systems use well-tested semi-empirical and ab-initio PESs by Varandas and Pais [17] and Sayós et al. [48], respectively. One can notice that the utilization of a semi-empirical PES does not necessarily lead to a lower computational cost of the QCT method, compared with the analytical fit to the ab-initio data. Lastly, the present paper focuses on O_2–N_2 collisions using the

latest available PES by Varga et al. [31]. This study is in progress and results are reported only for selected vibrational states.

An extensive overview of three- and four-body QCT methods is given elsewhere [42,49]. The present paper concentrates on kinetic models of hypersonic flows and provides discussion on utilization of the QCT data. The primary tool for analysis of state-specific RCs is the system of master equations. The general appearance of the kinetic model that includes the bound–bound and bound–free (dissociation and tunneling) processes is given by Eq. (1):

$$\frac{dn_i}{dt} = \sum_{i' \neq i}(K_{i' \to i} n_x n_{i'} - K_{i \to i'} n_x n_i) - D_i n_i n_x + R_i n_O^2 n_x$$
$$- T_i^f n_i + T_i^b n_O^2, \quad i = 1, \ldots, N \quad (1)$$

where n_i is the population of the i rovibrational state, $K_{i' \to i}$ is the rate of transition from i' to i rovibrational states, n_x is the number density of the collision partner of the O_2 molecule, D_i and R_i are the state-specific dissociation and recombination rate coefficients of the i state, T_i^f and T_i^b are the forward and backward tunneling rate coefficients, and N denotes the total number of rovibrational states. The summation in Eq. (1) is performed over the entire rovibrational ladder. The principle of detailed balance is invoked to generate rates of endothermic transitions to reduce the statistical error of the QCT method.

The rates of bound–bound and bound–free transitions can be averaged over the range of transrotational temperatures, because this type of thermal equilibrium is typically observed in gas flows with temperatures below 10,000 K. The system of master equations that employs rotationally averaged RCs is termed as the VT model. Otherwise, when a complete set of rovibrationally resolved RCs is used, the system of master equations is termed the RVT model.

The state-resolved approach becomes prohibitively expensive with increasing number of diatomic species and dimensionality of the problem. Although reduced-order models that retain the main features of the state-resolved approach have been proposed recently [50], the multitemperature (MT) model remains popular due to its simplicity. The solution of master equations provides new insight on parameters that are used in MT models. The present paper addresses the question of efficient utilization of the master equation results. The MT model, when formulated for simple heat bath conditions, consists of the following equations:

$$\begin{cases} \frac{\partial(\rho e_v)}{\partial t} = \rho_{O_2} \frac{e_v^\star - e_v}{\tau_v} + \dot{\omega}_{O_2} C_{DV} D_e \\ \dot{\omega}_{O_2} = R n_O^2 n_x - D(T_a) n_{O_2} n_x \end{cases} \quad (2)$$

In Eq. (2), e_v and $e_v^\star$ are the O_2 vibrational energy evaluated at T_v and T, respectively, ρ and ρ_{O_2} are the density of the O_2–O mixture and partial density of O_2, D_e is the classical dissociation energy, τ_v is the vibrational relaxation time, and $\dot{\omega}_{O_2}$ is the rate of O_2 generation. According to Park's model [51], the forward RC is computed using the governing temperature $T_a = \sqrt{T T_v}$. The recombination RC is computed through the equilibrium constant K_{eq} using the curve fit parameters provided in [51]: $R = D(T_a)/K_{eq}(T)$. The vibrational energy coupling coefficient C_{DV} corresponds to the loss of vibrational energy normalized by the classical dissociation energy. The system of Eq. (2) describes the transfer of vibrational energy assuming rotational equilibrium.

Lastly, one should discuss how the adjustable parameters, namely, τ_v, D, and C_{DV}, can be obtained from the system of master equations.

Table 1   Summary of QCT modeling effort

System	No. of states	Temperatures studied, K × 10^{-3}	No. of transitions	Computational time, h	Total no. of trajectories	Source
O_2–Ar	5117, $v_{max} = 36$	3–20	6.45 million	1.08×10^5	3.8×10^9	[44,46]
O_2–O	6245, $v_{max} = 46$	0.5–20	9.66 million	1.22×10^6	8.2×10^9	[20]
O_2–N	6136, $v_{max} = 43$	0.5–20	9.28 million	7.20×10^5	1.2×10^{10}	[47]
O_2–N_2	$N_2 - 9141$, $v_{max} = 53$; $O_2 - 5945$, $v_{max} = 35$	1–10	In progress	4.32×10^5	1.4×10^8	Present

The vibrational relaxation time, when the complete set of state-specific RCs is available, is obtained by the e-folding method [52]. When such a set of RCs is not available, the relaxation time can be derived from the rate of monoquantum deactivation from the first excited vibrational state, as is done for the O_2–N_2 system in the present work. This relaxation parameter does not account for the contribution of multiquantum jumps and excited vibrational states, for which the relaxation is usually faster than that for $v = 1$.

The dissociation RC, measured in shock-tube experiments, should be referred to as the quasi-stationary dissociation RC. Vibrational thermalization at the moment of onset of dissociation is incomplete, and the QSS dissociation RC is lower than the RC estimated at thermal equilibrium conditions. Hence, it is necessary to reevaluate the QSS dissociation RC as if the vibrational ladder is populated at $T_v = T$. According to Shatalov [53], D^{QSS} and D^{eq} are related through the following empirical relation:

$$D^{QSS} = D^{eq} \frac{T}{T_v} \exp\left(\frac{\tilde{D}}{RT} \left(\frac{1}{T} - \frac{1}{T_v} \right) \right) \qquad (3)$$

where parameter $\tilde{D} = D_e - \beta RT$ describes the average loss of vibrational energy due to dissociation. The recommended range of β is between one and two, and in the present work, β is set to 3/2.

The average loss of internal energy C_{DV} is estimated as a product of the state-specific dissociation and recombination RCs and the instantaneous populations of corresponding vibrational states [6]. The master equation approach generates time-dependent profiles of C_{DV} that can be used to improve the accuracy of the conventional MT approach in which a constant value of C_{DV} is assumed throughout the relaxation process.

III. Results

A. O_2–O

The interaction of the oxygen molecule with the parent atom is important, not only for the kinetics of hypersonic flow, but also in the chemistry of the upper atmosphere. Although ozone is present only in trace amounts, the strong absorptive properties of harmful UV radiation serve as motivation for the extensive study of ozone during the last several decades [1]. Because this type of interaction involves open-shell electrons, a rigorous quantum-mechanical treatment of the O_3 complex presents a great challenge. One of the main problems associated with the study of O_3 electronic structure is the presence of a potential barrier in the entrance/exit channel of the O_2–O collision. The existence or absence of such a reef structure is known to be responsible for the negative temperature dependence of rates at room temperatures. Although extensive quantum-mechanical studies of ozone in the ground electronic state indicate the existence of a small potential barrier, the trajectory studies using PESs that include such a barrier underestimate experimental rates. When the potential barrier is artificially removed, the experimental data are reproduced accurately. On the other hand, the semi-empirical PES by Varandas and Pais, obtained by the double many-body expansion method [17], has no potential barrier. Rates, obtained on the Varandas and Pais PES, match the experimental data quite accurately. For this reason, the Varandas and Pais PES was used recently to generate a complete set of state-specific transition rates for each internal energy level of oxygen at temperatures between 500 and 20,000 K [20,21]. In this section, the results of the master equation study of this system are reviewed and compared with the widely adopted multitemperature models.

1. Vibrational and Rotational Relaxation Times

Experimental investigation of oxygen vibrational relaxation in collisions with atomic oxygen was performed for room temperatures [54,55] as well as at moderate hypersonic temperatures between 1000 and 3500 K [56,57]. These data are summarized in Fig. 1, along with the computed vibrational and rotational relaxation times. These parameters are obtained from the solution of master equations coupled to the set of state-specific rates. In the presence of rotational
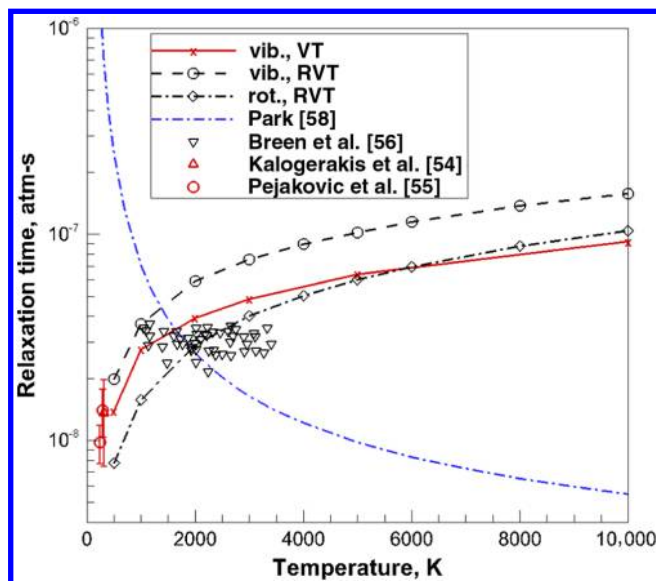

Fig. 1 Vibrational and rotational relaxation times if O_2–O collisions.

equilibrium, the VT thermodynamic model provides τ_v, given by a solid line in Fig. 1. The RVT model gives τ_v and τ_r, shown by dashed and dashed-dotted lines in Fig. 1. For reference, the Millikan–White (MW) [58] vibrational relaxation time, with parameters obtained by Park [59] by fitting to the measurements by Kiefer and Lutz [57], is shown by the dashed-dotted line. Error bars of QCT results are less than the symbol size.

Experimental data by Breen et al. [56] was obtained in a conventional shock tube with oxygen atoms generated by an RF discharge in either pure O_2 or an O_2/Ar mixture. Although this technique eliminated uncertainties arising due to ozone thermal decomposition, which serves as a source of oxygen radicals in the work by Kiefer and Lutz [57], Breen et al.'s data [56] are still much scattered. These measurements alone do not allow one to make a conclusion about agreement in temperature dependence of τ_v between QCT data and experiments. Nevertheless, measurements conducted by Pejaković et al. at room temperature [55] clearly indicate that O_2–O vibrational relaxation becomes less efficient with temperature, as predicted by the master equation simulations. The MW τ_v fails to describe the rapid relaxation at low temperatures. This is due to the inapplicability of the Landau–Teller theory to molecular systems that form metastable chemical bonds. Although the question of existence of a barrier in O_3 is not completely settled, the presence of a subtle repulsion in the O_3 entrance/exit channel should have a minor influence on τ_v at temperatures relevant to hypersonic flows.

The vibrational relaxation time in the RVT model is larger than that in the VT model due to the presence of significant rotational nonequilibrium in the considered temperature range. Typically, τ_r is assumed to be much shorter than τ_v at low to moderate hypersonic temperatures [60]. This is not the case for thermalization of internal modes that occurs only via O_2–O collisions. In fact, if only O_2–O collisions are considered to contribute in relaxation, the rotational and vibrational modes should be treated simultaneously because τ_v and τ_r, obtained via the RVT model, are different by a factor of 2 at maximum. In experiments by Breen et al. [56], the molar fraction of atomic oxygen did not exceed 1.84%, hence the effect of O_2–O rotational nonequilibrium should be minimal under these conditions.

Because thermal relaxation and dissociation occur at different timescales, it is possible to consider these two phenomena separately when modeling nonequilibrium chemical reactions at moderate temperatures. However, as temperature increases, the dissociation may start before the complete thermalization of the rovibrational ladder. The complete set of O_2–O QCT transition rates supplemented by the O_2–O_2 set of forced harmonic oscillator (FHO) transition rates was used previously to model vibrational relaxation in shock waves at velocities between 3.07 and 4.44 km/s [61]. These simulations were motivated by recent experimental measurements of laser absorption
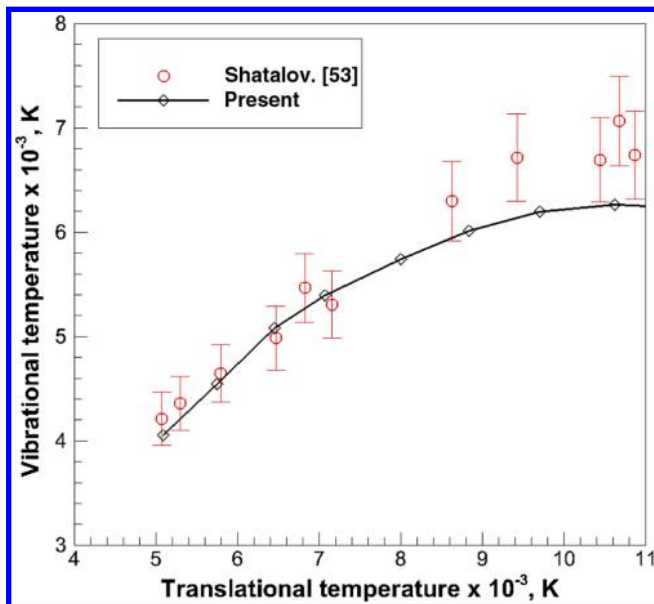
Fig. 2   Variation of vibrational temperature behind the shock front with T.

Fig. 3   Equilibrium and QSS dissociation RCs in O_2–O collisions.

in the Schumann–Runge (SR) bands [62]. In these experiments, the absorption of laser radiation at several wavelengths between 230 and 260 nm was interpreted in terms of translational and vibrational temperatures of the nonequilibrium gas. Bound–bound and bound–continuum transitions from $^3X_g^-$ to $B^3\Sigma_u^-$ state were considered for all vibrational states, assuming a Boltzmann population of energy levels [63]. One should note that, due to the multitemperature assumption used in [63] to estimate the absorption coefficient, the comparison of experimental data and the state-to-state (STS) model should be done with caution.

The vibrational temperature observed before the onset of dissociation is shown in Fig. 2. The horizontal scale corresponds to the maximum of translational temperature, registered immediately after the shock wave arrives at the optical station. At moderate nonequilibrium conditions, the state-resolved model predicts the vibrational temperature during the quasi-steady regime quite accurately. As temperature increases further, the present model slightly (200–500 K) underestimates the measurements. The disagreement may be caused by uncertainties in the experimental approach related to the non-Boltzmann population of vibrational states as well as due to inaccuracies of the FHO model used to describe O_2–O_2 collisions. It is highly desired to repeat the calculations conducted in [61] when a complete set of O_2–O_2 RCs generated on accurate PESs become available.

2.   Dissociation Rate Coefficient

The master equation approach provides a time-dependent evolution of the rovibrational distribution. It is possible to define a dissociation rate that takes place during the QSS phase (i.e., when the condition $d\varepsilon_v/dt = 0$ is held). Because the experimental measurements can only access a depletion rate during the QSS phase, the similar result from the master equation simulation is of great importance because it allows direct comparison between theory and experiment.

The QSS dissociation RC for O_2–O collisions is shown in Fig. 3. Three curves with square, circular, and diamond symbols represent RCs estimated under thermal equilibrium conditions (i.e., when $T = T_v = T_r$), as well as during the QSS phase using the VT and RVT models, respectively. For comparison, the experimental measurements are shown by triangular symbols. Also, the Park [51] dissociation rate coefficient D_{Park} is shown by a dashed-dotted line. These data are obtained by computing an effective temperature $T_a = \sqrt{TT_v}$, where vibrational temperature is taken during the QSS phase from heat bath simulations, accounting for both O_2–O and O_2–O_2 collisions [64].

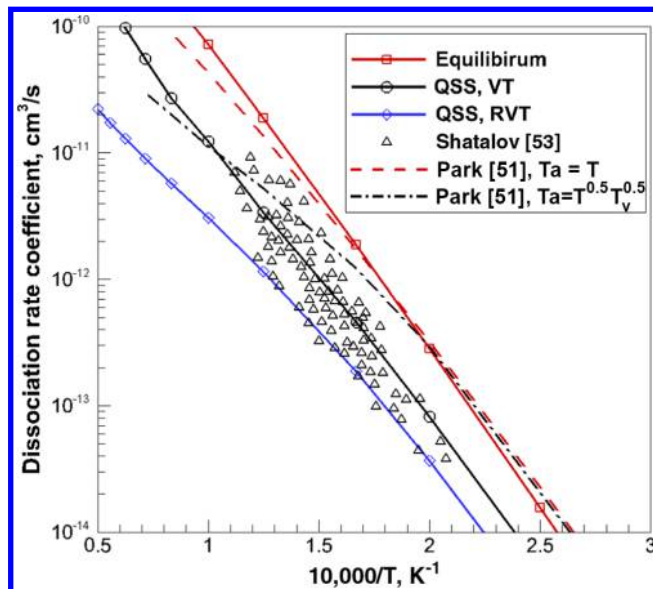At low translational temperatures, when the QSS vibrational temperature reaches equilibrium conditions, D_{Park} and D_{eq} RCs are in good agreement. However, the QSS dissociation RC is substantially lower than the equilibrium RC. This is because vibrationally excited states that contribute to the dissociation are underpopulated compared with the equilibrium distribution at given T_v. This can be clearly seen from Fig. 4. The cumulative sum of dissociation probability, computed as the product of state-specific population and the corresponding dissociation RC, significantly depends on the contribution of excited vibrational states. The deviation from equilibrium population can be observed for $v > 15 \times (e_v = 2.4$ eV$)$. These states contribute more than 60% in the dissociation probability function. Thus, the depletion rate, computed at the vibrational temperature of the QSS phase, overestimates the actual dissociation rate.

The Park [51] dissociation RC, estimated at T_a, is noticeably higher than the QSS RC at temperatures below 8000 K. At higher temperatures, the Park [51] RC fits the upper interval of experimental data, however, agreement with the QSS VT RC is not achieved. The following section shows that the use of the QSS dissociation RC without traditional coupling by means of T_a produces accurate results when incorporated in the MT model.
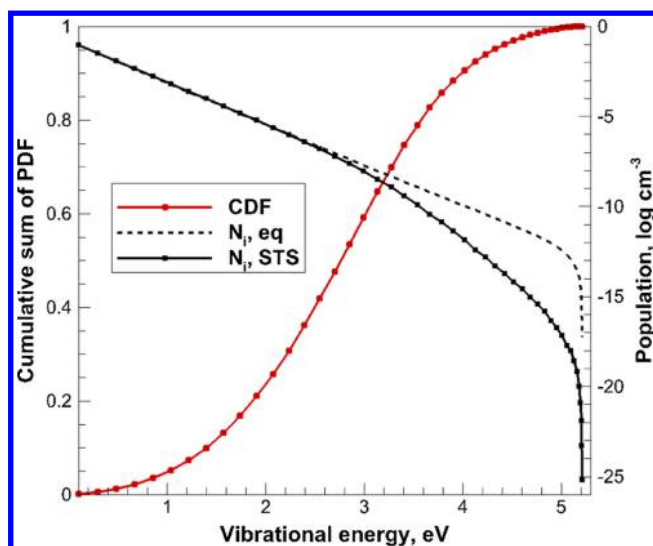

Fig. 4   Cumulative distribution function (CDF) and population of vibrational ladder during the QSS phase, $T = 5000$ K (PDF, probability distribution function).

3. Comparison of State-to-State and MT Methods

Because of the high cost of the STS approach, there is a potential interest to use the information about nonequilibrium populations and state-specific rates to improve the accuracy of the simple and efficient MT approach. In the present work, the solutions from the STS and MT models are compared side-by-side for an ideal heat bath of oxygen at translational temperatures of 5000; 8000; 10,000; and 14,000 K. There are three primary parameters that can be adjusted to fit the solution of the MT approach to that of the STS method. Namely, these are the vibrational relaxation time, dissociation rate coefficient, and the average loss of internal energy due to dissociation. It was shown recently [20] that the O_2–O e-folding relaxation time accurately describes the evolution of vibrational energy when incorporated in the Landau–Teller (LT) equation. Therefore, it is decided to keep the LT term and vibrational relaxation time unadjusted.

The appropriate adjustment of dissociation RC and vibration–dissociation coupling in the MT model parameter should be based on the temporal evolution of these parameters during thermalization. In heating flows, the rate of dissociation is often much larger than the rate of recombination, especially at early stages of thermalization. It is possible to neglect the recombination and define the macroscopic instantaneous dissociation RC in the following manner:

$$D^{inst} = \frac{\dot{\omega}_{O_2}}{n_{O_2} n_O} \qquad (4)$$

The O_2–O instantaneous and QSS dissociation RCs and the vibration–dissociation coupling parameter are shown for considered heat bath conditions in Figs. 5 and 6. In Fig. 5, the symboled lines correspond to the instantaneous RC computed as the ratio of difference in the O_2 number density and the time step, whereas dashed lines correspond to D^{QSS}. At low temperatures, the maximum of D^{inst} corresponds to the plateau at the QSS level. At higher temperatures, the QSS assumption breaks down and the QSS RC is bounded by some minimal and maximal values of instantaneous RCs, shifting toward the lower bound with increasing temperature. In fact, the differences between the minimum and maximum of instantaneous RCs becomes smaller at higher temperatures. One should note that Eq. (4) allows for zero dissociation RCs, which is, of course, unphysical. However, the rapid drop of D^{inst} is observed only after the QSS phase when a system is nearly at complete equilibrium, and so it is of little significance.
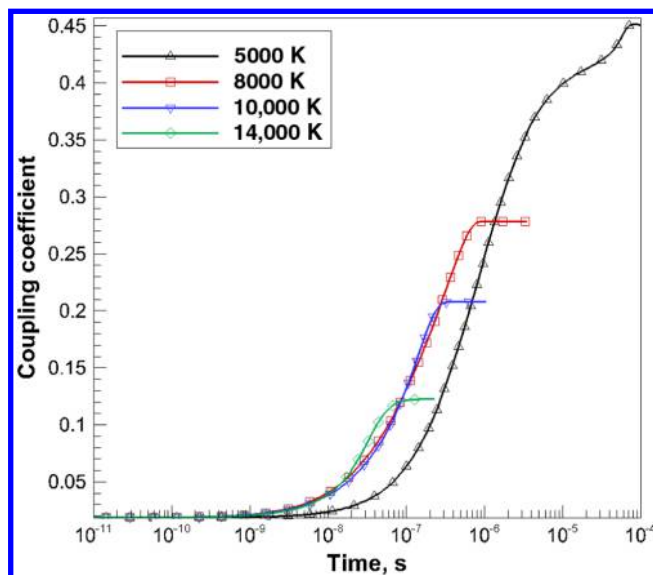
Fig. 6   Vibration–dissociation coupling parameter in O_2–O collisions.

Because little to no dissociation occurs at low temperatures before the QSS phase, it will be appropriate to assume $D(T_a) = D^{QSS}$ in the MT model. At higher temperatures, the dissociation occurs simultaneously with thermal relaxation, hence, again, it will be accurate to assume the QSS RC as the replacement for the actual dissociation RC in Eq. (2). The most pronounced inaccuracy in the modified MT model will be observed for intermediate temperatures.

Figure 6 illustrates that it is incorrect to assume a constant C_{DV} throughout the entire relaxation process. In fact, this coupling parameter has initially a very small value reaching a nearly constant level during the QSS phase and thereafter. For the sake of simplicity, a linear dependence of C_{DV} on T_v can be proposed:

$$C_{DV} = C_{DV}^{QSS} \times \min\left(\frac{T_v}{T_v^{QSS}}, 1\right) \qquad (5)$$

where C_{DV}^{QSS} and T_v^{QSS} are the vibration–dissociation coupling parameter and vibrational temperature during the QSS phase [20,62]. The comparison of the STS method and standard MT approach with dissociation rate, computed according to [51], was previously reported in [20] for temperatures of 5000 and 10,000 K. The comparison of STS, standard, and modified MT approaches is shown in Fig. 7 for translational temperatures of 5000; 8000; 10,000; and 14,000 K. The modified MT approach performs very adequately, compared with the standard MT model. As expected, the least successful agreement is observed for moderate temperatures.

B. O_2–N

The interaction of the oxygen molecule with nitrogen atoms is important in shock-heated air, the chemistry of the upper atmosphere, and the combustion of carbon-based fuels. The formation of nitric oxide in these applications occurs via the Zeldovich mechanism. However, the O_2–N nonreactive channel of the interaction can also be important in modeling flows with a large number of nitrogen atoms. State-specific data on O_2–N collisions become necessary when developing high-fidelity thermochemistry models of nonequilibrium hypersonic flows. Meanwhile, O_2–N collisions are known to occur on multiple PESs of different multiplicity [48]. The lowest 2A′ PES has a relatively low potential barrier of approximately 0.3 eV and a deep potential minimum that corresponds to $NO_2(X^2A_1)$. To the authors' knowledge, a model of oxygen relaxation in collisions with nitrogen atoms has not been proposed previously.

The experimental study of the O_2–N system is complicated due to the large difference in dissociation energies of oxygen and nitrogen molecules. The presence of fast chemical reactions involving nitric oxide also complicates measurements of the vibrational distribution
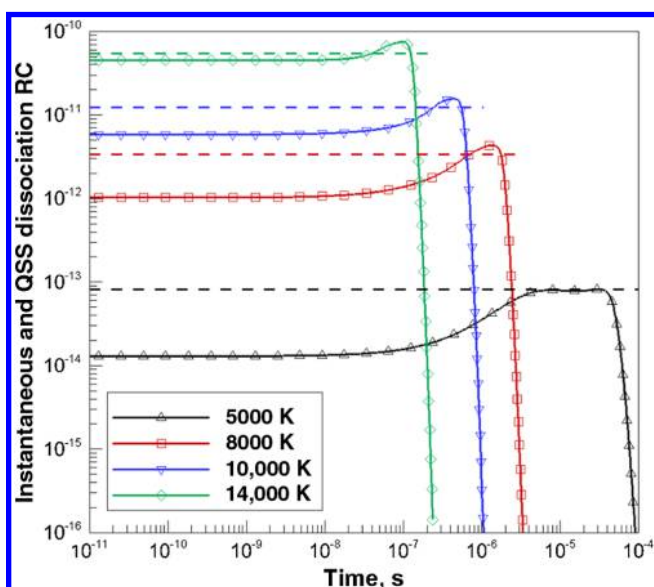

Fig. 5   Instantaneous and QSS dissociation RCs in O_2–O collisions; solid lines describe RC obtained via Eq. (4) and dashed lines correspond to QSS RC.
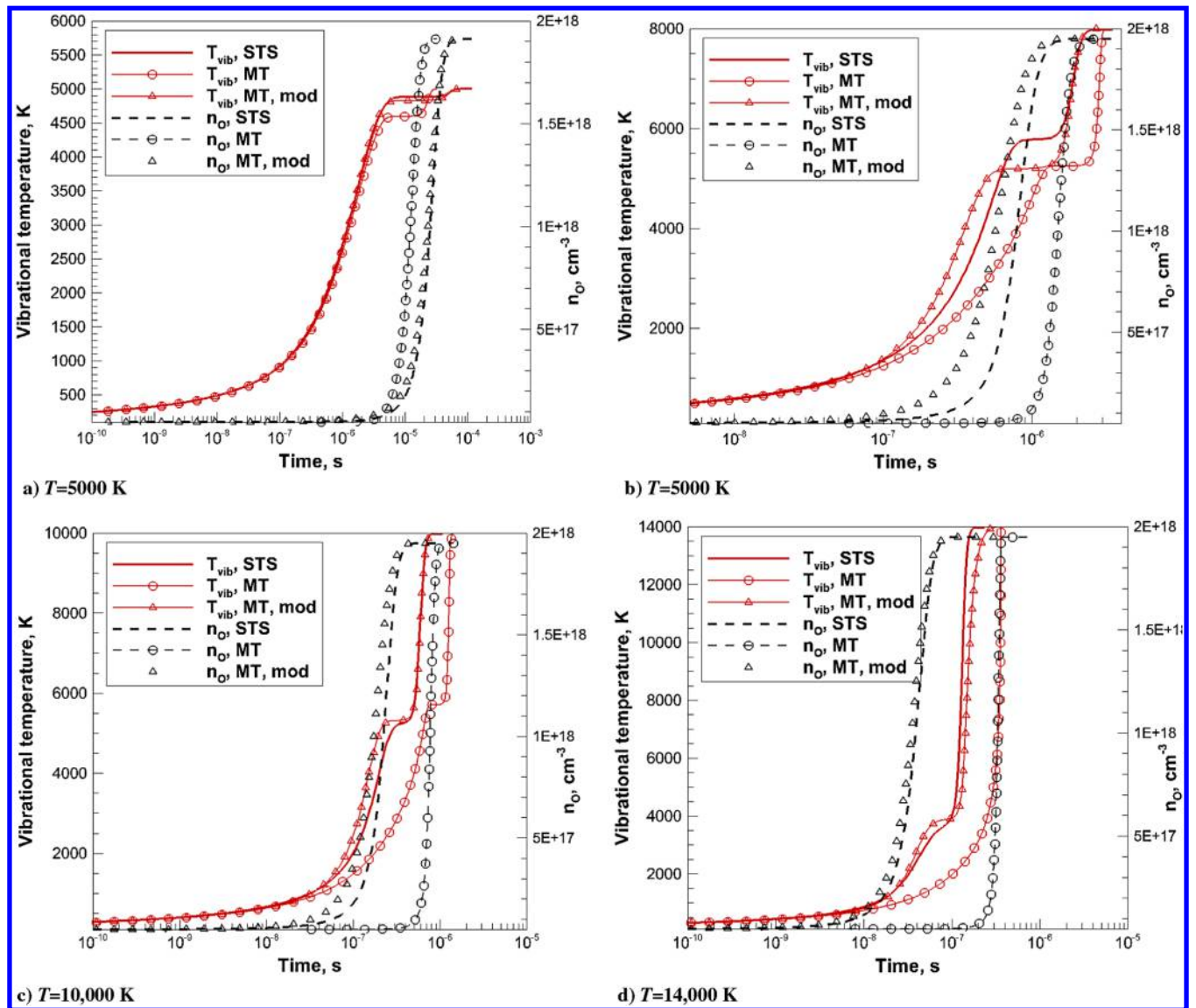
a) $T=5000$ K

b) $T=5000$ K

c) $T=10,000$ K

d) $T=14,000$ K

Fig. 7   Comparison of STS and modified MT approaches.

of products. As a result, experimental data on oxygen relaxation in O_2–N collisions are absent. To overcome this difficulty, an equality of relaxation times in O_2–N and N_2–O collisions has been assumed in computational models of hypersonic flows [65]. Although this assumption can be partially justified due to the similar masses of reactants, state-to-state reaction rates are desirable for the implementation of more accurate state-resolved models of hypersonic flows.

The O_2–N vibrational and rotational relaxation times, obtained via the solution of master equations, are shown in Fig. 8. For reference, the experimental data for the N_2–O system [66–68] are shown by symbols. Eckstrom [66] and Breshears and Bird [68] used thermal decomposition of ozone in shock-tube experiments. In the former work, carbon monoxide was used as a tracer of vibrationally exited nitrogen due to fast energy exchange between these two species. The later work adopted a laser schlieren technique, similar to [57], to derive the relaxation time from the postshock density gradient. The main source of uncertainty in these works comes from the presence of impurities and from the ozone decomposition stoichiometry. The data by Eckstrom [66] was estimated to have 50% uncertainty. At lower temperatures, McNeal et al. [67] used a photoionization detector to measure the rate of vibrationally excited nitrogen in the afterglow. All these works have reported much faster relaxation of nitrogen compared with the Landau–Teller theory, which was
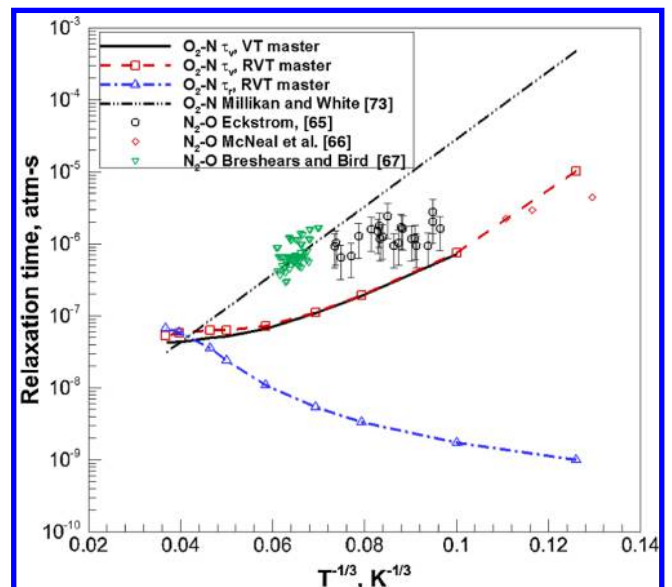

Fig. 8   Vibrational and rotational relaxation times in O_2–N and N_2–O collisions.

attributed to the presence of chemical effect in the metastable N_2O complex.

As one can see, the present QCT results for O_2–$N\tau_v$ lay lower than N_2–$O\tau_v$. The Millikan–White [58] correlation provides a substantially higher estimation of τ_v as well, indicating that, in O_2–N collisions, the chemical effect may also be important. Because the experimental approach disregarded the presence of rotational nonequilibrium, the measurements should be compared with the results of the VT model. Unlike in O_2–O collisions, rotational thermalization in O_2–N occurs more rapidly than vibrational relaxation up to 8000 K. Hence, the assumption of rotational equilibrium is valid at lower temperatures.

Thermal equilibrium and QSS dissociation RCs in O_2–N collisions are shown in Fig. 9. For reference, the previously recommended two-temperature dissociation RC [59] is shown by symbols. The previous O_2–N dissociation RC [51] is simply assumed to be equal to the O_2–O RC, because there is no experimental data available for the former molecular system. In the present work, the Park [51] O_2–N RC is estimated at T_a, calculated using the QSS vibrational temperature of the O_2 rovibrational manifold in a heat bath of nitrogen atoms [47]. Similar to O_2–O collisions, the Park [51] dissociation RC overestimates the QSS depletion RC, given by solid and dashed-dotted lines for the RVT and VT models. This is due to incomplete thermalization of the ladder during the QSS phase, even at low temperatures of the heat bath. The Park [51] RC is also higher than the equilibrium RC, derived in the present study, indicating that the dissociation in O_2–O collisions proceeds more efficiently than in the O_2–N system. Unlike in O_2–O collisions, the difference in QSS VT and RVT RCs is quite small for low temperatures. This is due to the effect of nearly complete rotational equilibrium that occurs before the onset of dissociation. As expected, the difference between D_{QSS}^{RVT} and D_{QSS}^{VT} increases at high temperatures.

The instantaneous dissociation RC, computed from Eq. (4), is shown in Fig. 10 for temperatures of 5000; 8000; 10,000; and 14,000 K, along with the QSS dissociation RC, previously reported in [47]. As in the case of O_2–O collisions, the O_2–N instantaneous dissociation RC is not constant throughout the relaxation, due to varying state-specific dissociation RCs of different energy levels and evolving rovibrational distribution in time. D^{inst} levels off with D^{QSS} at temperatures as high as 10,000 K, whereas in O_2–O collisions, this occurs at 5000 K. The difference between minimal and maximal instantaneous RCs for the O_2–N system is significantly larger than for the O_2–O system. For instance, the O_2–O instantaneous RC increases between 1.22 and 6.1 times during relaxation in the range of temperatures between 5000 and 14,000 K. For O_2–N, this increase is
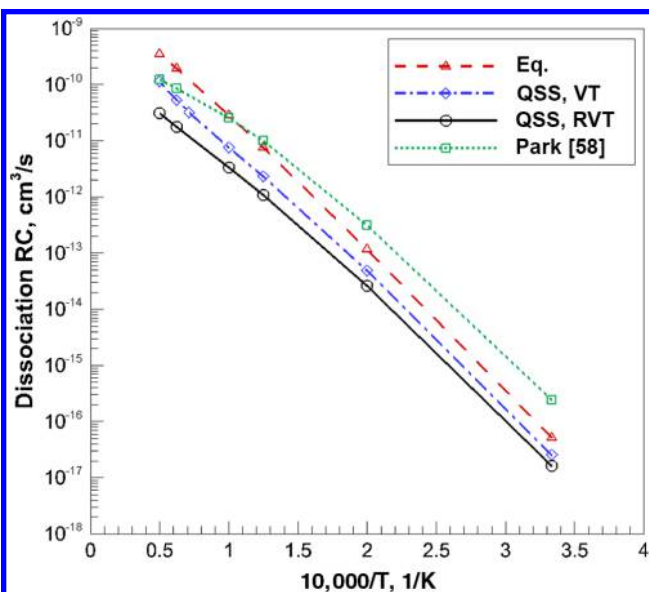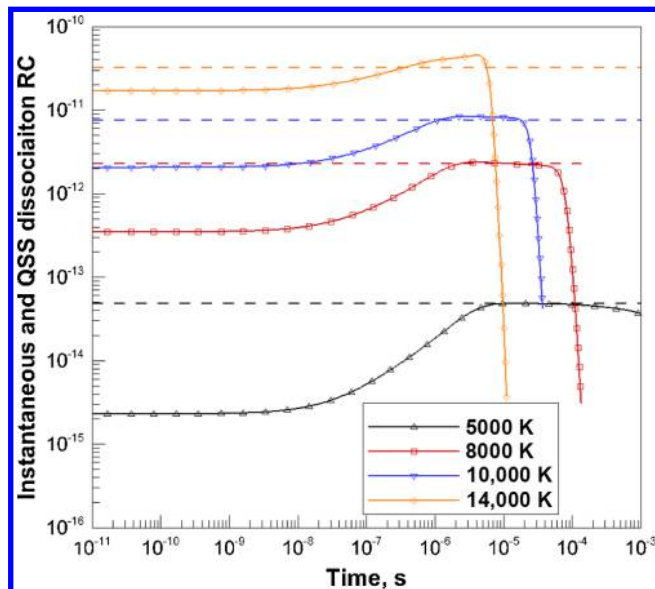

Fig. 10 Instantaneous and QSS dissociation RCs in O_2–N collisions.

between 2.07 and 20.69 times for a similar temperature range. This can be attributed to the efficient "scrambling" of precollisional states in O_2–O and the large probability of exchange reaction even for low-lying vibrational states. As was discussed previously [1], this type of interaction is due to the small O_3 potential barrier. The exchange reaction in O_2–N collisions leads to products other than reactants and does not contribute to the relaxation of oxygen.

The simple use of the QSS RC in the O_2–N MT model, as was done for O_2–O, would lead to an overestimation of the actual RC. To accurately match the solution of master equations, the dissociation RC in the MT model should be modified. From the temporal evolution of instantaneous RCs, one can see that it varies between D_{min} and roughly D_{QSS}, rapidly increasing at some vibrational temperature that is below the QSS T_v. The following factor accounts for the variation of RCs due to nonequilibrium population of the vibrational ladder:

$$\psi = (D_{QSS} - D_{min})\left[\frac{1}{\pi}a\tan\left(\alpha\left(1 - \frac{T_v^0}{T_v}\right)\right) + \frac{1}{2}\right] + D_{min} \quad (6)$$

Similar to Eq. (6), the nonequilibrium factor was proposed in [69] for a mixture of N_2 and N. In the original work by Valentini and Schwartzentruber [69], the lower bound of ψ is set to zero. In the present work, the effect of initial dissociation that may take place at high temperatures before the QSS phase is taken into account by limiting the lowest value of ψ at D_{min} level. In fact, D_{min} does not depend on the number density of O_2 or N and is defined only by T and T_v. For the variation of initial vibrational temperature T_v between 100 and 1000 K, it is found that D_{min} varies not more than 10%. The adjustable parameter that triggers dissociation T_v^0 should be chosen for each molecular species individually. For oxygen, in the present work, it is set to 3000 K. The parameter of steepness α is set to two.

The number density of atomic oxygen and T_v, generated by the STS, conventional, and modified MT models are shown in Fig. 11. Indeed, the modification of the MT model with Eq. (6) significantly improves the agreement in species number density at lower temperatures, compared with the standard MT approach. At higher temperatures, the composition is similar for the modified MT and STS methods because the variation of the instantaneous RC is relatively small and the actually RC is quite close to D^{QSS}. Overall, the modification of C^{DV} and D^{QSS} reflected in Eqs. (5) and (6) substantially improves the quality of the MT solution when compared with the reference STS approach.
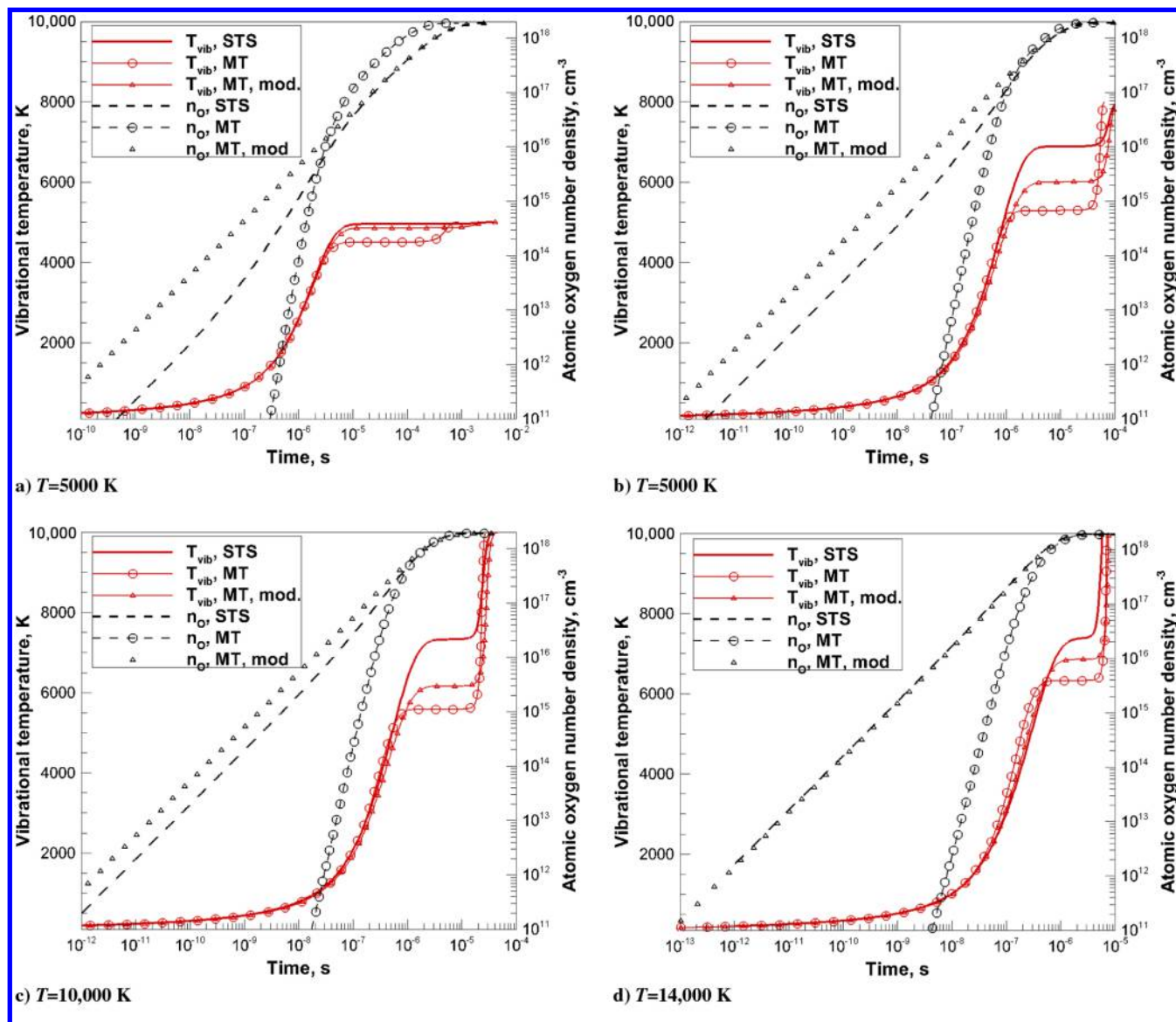

Fig. 9 Thermal equilibrium, QSS VT and RVT dissociation RCs in O_2–N collisions.

Fig. 11   Comparison of STS and modified MT approaches for O_2–N heat bath simulation.

C. $O_2 - N_2$

The interaction of O_2 with molecular nitrogen is of great importance in hypersonic thermochemistry due to the large difference in the dissociation energy of these species. There are several PESs in the literature that describe the N_2O_2 system. One of the first N_2O_2 PESs was proposed by Aquilanti et al. [2] for studying rigid molecules in their ground vibrational state. This PES was designed specifically for methods of molecular dynamics for the upper atmosphere, however, it has a little use for aerothermodynamics. Bartolomei et al. [70] recently published an improved ab-initio PES with similar restrictions. The VT and VV energy transfer was studied by a semiclassical coupled method by Billing on an empirical PES in the range of temperatures between 250 and 1000 K [26]. Recently, Garcia et al. [45] reported VT and VV rate coefficients using an improved PES for selected vibrational states of oxygen at temperatures up to 7000 K. This PES is based on ab-initio calculations that are interpreted as a combination of bond–bond interactions, namely, van der Waals and electrostatic interaction terms. Unfortunately, the dataset reported in [45] is incomplete and, thus, a master equation simulation still cannot be performed.

An analytical fit to the global ab-initio PES of triplet N_2O_2 was recently published by Varga et al. [31]. This PES was obtained by multistate complete-active space second-order perturbation theory and was specifically designed to describe collisions at high kinetic

energies. Most of the multireference calculations of electron correlation energy were conducted in the range of potential energies between 100 and 350 kcal/mol (76% of the total 54,889 data points). It is worth noting that the long-range forces are not described correctly in this PES, thus it may not be suitable for low energy collisions. The following section compares the rate coefficients, generated by trajectory simulations on this PES, with the existing theoretical and experimental data.

1.   VT and VV Rate Coefficients

Rates of VV and VT energy transfer for $O_2(v = 25)$ were computed by Garcia et al. [45] on two PESs of different fidelity using the SC and QCT methods. In the present work, rate coefficients in [45] are compared with those obtained by the QCT method on the PES of Varga et al. [31]. The VT reaction corresponds to the mono- and double-quantum deactivation of oxygen with nitrogen remaining in the same vibrational state. The VV reaction is described by O_2 monoquantum deactivation with the simultaneous single quantum activation of nitrogen. Rate coefficients of these processes are shown in Table 2.

The present QCT results agree better with the data, obtained on the Garcia et al. [45] PES, based on ab-initio data, than with the data generated using the simpler Billing [26] PES. This is observed for all three types of considered transitions. In fact, the Billing PES produces a systematic overestimation of rates, which may be

Table 2 Vibration-vibration and vibration-translation transition RCs in $O_2(v = 25) - N_2$, in cubic centimeters per second, at $T = T_r = 1000$ K

Source	Transition	Rate coefficient
QCT, Present	$O_2(v - 1) + N_2(w)$	4.36×10^{-12}
QCT, Garcia et al. PES [45]	— —	2.3×10^{-12}
SC, Garcia et al. PES [45]	— —	1.1×10^{-12}
QCT, Billing PES [26]	— —	1.2×10^{-11}
SC, Billing PES [26]	— —	3.5×10^{-12}
QCT, Present	$O_2(v - 2) + N_2(w)$	8.16×10^{-14}
QCT, Garcia et al. PES [45]	— —	1.1×10^{-13}
SC, Garcia et al. PES [45]	— —	6.0×10^{-14}
QCT, Billing PES [26]	— —	1.5×10^{-12}
SC, Billing PES [26]	— —	3.9×10^{-13}
QCT, Present	$O_2(v - 1) + N_2(w + 1)$	2.17×10^{-15}
SC, Garcia et al. PES [45]	— —	1.6×10^{-17}
SC, Billing PES [26]	— —	3.7×10^{-16}

explained by the fact that this PES is more repulsive than the Garcia et al. [45] ab-initio PES, and the attraction in N_2O_2 dimer configuration in the Billing PES is less pronounced. As expected, the rates of VT transition, generated in the present work, generally agree better with the results of QCT calculations than with the SC method.

The situation of energy transfer in collisions with oxygen in the ground vibrational states is drastically different. The VT and VV rates of energy exchange in $O_2(v = 0) + N_2(w = 1)$ are shown in Fig. 12. VV RCs correspond to the products $O_2(v' = 1) + N_2(w' = 0)$, whereas the VT RCs describe the production of $O_2(v' = 0) + N_2(w' = 0)$. Results of SC calculations by Garcia et al. [45] are shown by empty symbols. An empirical rate of VV transition, derived by Gilmore et al. [71] from experimental data on transition probabilities of the VV exchange reaction [72,73], is shown by long dashed curve. The experimental approach combines generation of spark interferograms with the following analysis of density profiles, as well as the measurements of infrared emission from CO at 4.6μ of wavelength, used as a tracer for the N_2 population. The last fact can be justified taking into account the very close fundamental vibrational frequencies of N_2 and CO.

Two important conclusions can be derived from this comparison. First, the agreement between SC and QCT approaches is satisfactory only at temperatures higher than 3000 K. Below this temperature, the QCT method strongly underestimates the RC of VV and VT reactions, compared with the result of SC calculations. There are two possible explanations for this disagreement. First, the QCT and SC calculations were conducted on two different O_2N_2 PESs. Although

the difference between these two methods in Table 2 is not as large as for the RCs involving $O_2(v = 0)$ in Fig. 12, only SC calculations on the PES given in [31] could provide an explanation for this difference.

Second, there is a possibility for the failure of the QCT method at low temperatures due to pronounced influence of quantum effects. Previously, it was shown that the QCT approach severely underestimates the RC of $O_2(v = 1)$ monoquantum deactivation in collisions with Ar at hypersonic temperatures [44]. These differences cannot be explained by statistical uncertainty of the results. Similar to O_2–Ar, the QCT method in the present work underestimates selected RCs compared with the SC method that adopts a quantal treatment of the vibrational mode.

Another important observation is related to the disagreement in VV RCs between the SC method and experimental data. This may be attributed to some uncertainties in the PES, used in [45], as well as to the theoretical interpretation of experimental data. Indeed, the analysis of interferograms in [72,73] was outlined assuming that the relaxation of nitrogen in the O_2–N_2 mixture can be represented as a superposition of two processes with different timescales. During a short period of time after the shock passage, oxygen quickly relaxes in collisions with N_2 and O_2 molecules via the VT energy transfer mechanism. After molecular oxygen receives a sufficient amount of vibrational energy from the translational motion of the particles, the energy exchange between N_2 and O_2 starts to play a role. Moreover, in experimental work by White [72], it was assumed that the VT process of N_2 excitation in collisions with oxygen is noticeably slower than the N_2–O_2 VV process, and the latter process should be responsible for the rapid excitation of N_2 in air relative to pure N_2.

The experimental data on vibrational relaxation time in pure oxygen are well known [58] and can be interpreted in terms of the monoquantum deactivation RC form $O_2(v = 1)$. Such data are shown in Fig. 12 with a dashed-dotted line. Indeed, the RC of monoquantum deactivation in pure O_2 is substantially higher than either VT or VV RCs in $O_2(v = 0) + N_2(w = 1)$ collisions obtained via SC and QCT methods. However, the RCs of O_2–N_2 VV transition by Gilmore et al. [71] is comparable to the relaxation RC in pure oxygen and do not comply with the hypothesis about the two-stage N_2 relaxation process in air [72]. Moreover, the RC of VT process, given by empty and filled triangles, is higher than the RC of VV process obtained via the trajectory simulation approach. This indicates that the MW correlation rule for N_2–O_2 collisions, used in [72] to solve for the VV exchange RC, may not be accurate enough for the analysis of the experimental data. Clearly, the most rigorous approach would consist of analysis of interferograms, obtained in [72,73] using the new RCs obtained on accurate PES by means of trajectory propagation methods accounting for quantum effects.

2. Vibrational Relaxation and Dissociation of Oxygen

Because the QCT method is quite accurate in describing the vibrational energy exchange at high translational energies, it can be used for comparison of vibrational relaxation time, derived from the rate of monoquantum deactivation from the first excited vibrational state with existing experimental data. The cross section of monoquantum deactivation, averaged at transrotational temperatures between 4000 and 10,000 K is shown in Fig. 13. The vibrational relaxation times, derived from the cross sections in Fig. 13, are shown in Fig. 14. The dashed line corresponds to the Millikan–White [58] relation with parameters estimated from the vibrational frequency of oxygen and the reduced mass of colliding particles. It is important to note that the MW curve is not obtained by fitting the general expression to experimental results. Circular symbols correspond to O_2 vibrational relaxation times in collisions with N_2 measured in air and in a 5%O_2–95%N_2 mixture by Generalov and Losev [74]. The red line describes the present O_2 relaxation time obtained on the PES by Varga et al. [31].

The experimental data by Generalov and Losev [74] indicates a slower vibrational relaxation time of oxygen in collisions with N_2, compared with the empirical equation by Millikan and White [58]. This overestimation is very modest and probably falls in the uncertainty interval of 15–30% as stated in the original work [74]. The present QCT results are closer to the data of Generalov and Losev [74]
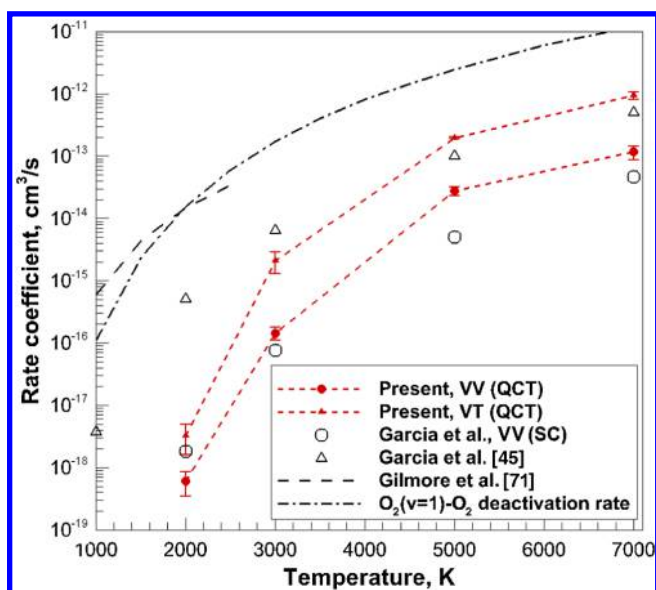

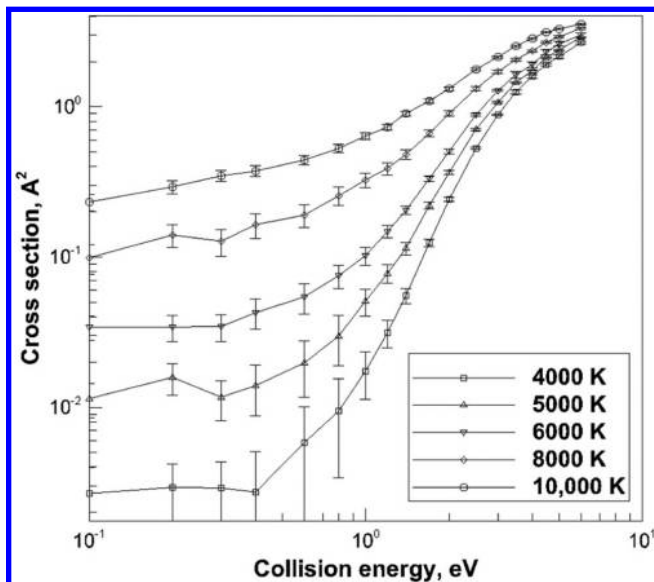**Fig. 12   Transition RCs of $O_2(v = 0) + N_2(w = 1)$ collision.**

Fig. 13 Cross sections of $O_2(v = 1) - N_2$ monoquantum vibrational deactivation, $T = T_r$.
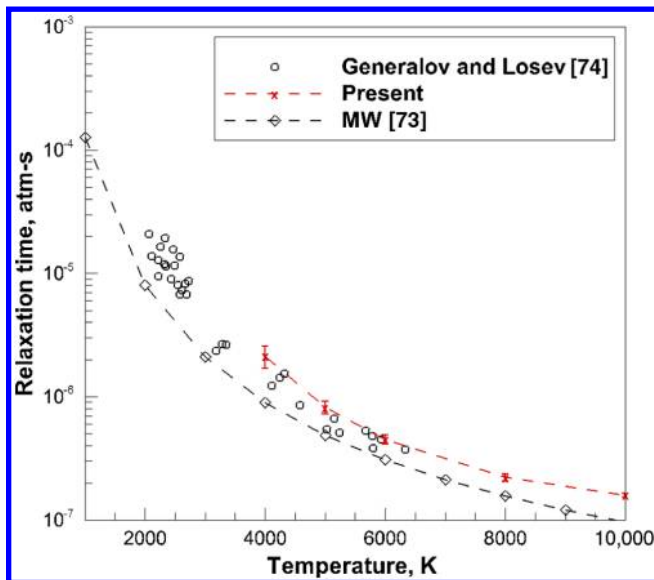

Fig. 14 Vibrational relaxation time of oxygen in collisions with N_2, $T = T_r$.

than to the MW equation. Overall, the present relaxation time is systematically higher than that predicted by the MW correlation. At higher temperatures, namely, at 10,000 K, larger disagreement is seen between the present and MW results. There are several reasons for this. The breakdown of the MW correlation at high temperatures was discussed previously [51]. The uncertainty in relaxation time, derived by means of the QCT method, is related to the accuracy of the PES, implemented in the trajectory simulations, accuracy of the QCT method itself, statistical accuracy, and details of the kinetic model. Although it is extremely difficult to quantify the influence of the first two factors, some things can be said about the influence of the kinetic model. The present relaxation time is derived based on the deactivation RC from the first excited vibrational state. Previous master equation simulations [20,47] for atom–molecule systems indicate that multiquantum processes and kinetics of higher vibrational states tend to decrease the relaxation time at temperatures larger than the characteristic vibrational temperature of the target molecule, which is approximately 2239 K for O_2. The master equation simulation of O_2–N_2 is of great interest and should be conducted in the future.

The dissociation rate of oxygen in collision with a nitrogen molecule was measured previously in shock-tube facilities [74–76].
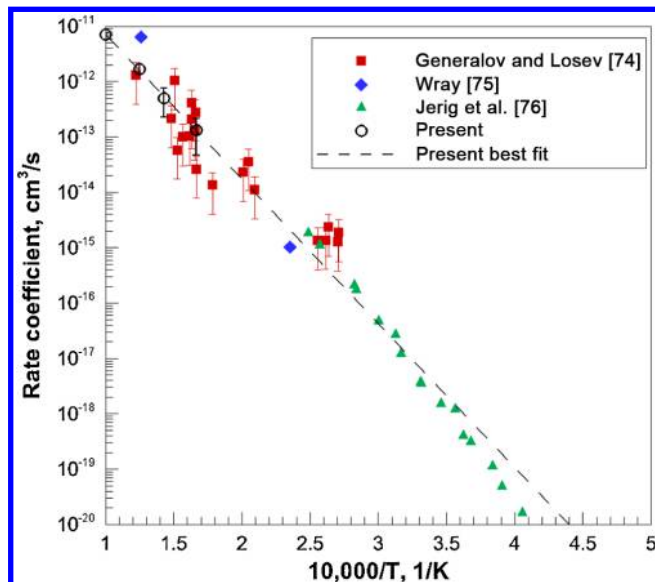

Fig. 15 Thermally equilibrium dissociation RC of oxygen in collisions with N_2.

In the work by Generalov and Losev [74], the rate of dissociation was derived from the initial slope of O_2 concentration after the quasi-stationary distribution was obtained. The rate of oxygen depletion was analyzed by absorption in the SR bands at the wavelength of 224.5 nm. These data are limited to the temperature range between 2700 and 7000 K. In the more recent work by Jerig et al. [76], the rate of dissociation was measured by means of atomic resonance absorption spectroscopy in the range of temperatures between 2400 and 4100 K. This method allows relatively accurate measurements of oxygen atomic concentration in the range of number densities between 10^{12}–10^{14} cm^{-3} at 130.5 nm of wavelength.

The thermal equilibrium dissociation RC of oxygen is shown in Fig. 15. Circular symbols describe the present QCT data, and the dashed line extrapolates the QCT D^{eq} at temperatures below 6000 K. Filled symbols correspond to D^{eq} obtained from the experimental measurements of D^{QSS} [74–76] by means of Eq. (3). As stated in [74], the experimental uncertainty of the dissociation RC, shown by square symbols, can be as high as 70–100%. The lower boundary of this interval is shown in Fig. 15 for the results of Generalov and Losev [74].

The present extrapolated results are in very good agreement with the measurements by Jerig et al. [76]. The shock-tube measurements by Generalov and Losev [74] have much larger scatter, however, the QCT RC is well within the uncertainty range. For extrapolation, the generalized Arrhenius form is used: $D^{eq} = AB^T \exp(-C/T)$. The corresponding coefficients for O_2–N_2 thermal equilibrium dissociation RC are found to be $A = 8.132 \times 10^{-10}$ cm^3/s, $B = -0.131$, $C = 59380$ K. This expression is valid for translational temperatures between 2000 and 10,000 K.

IV. Conclusions

A summary of QCT and master equation studies for O_2–O, O_2–N, and O_2–N_2 molecular systems is given in the present paper. The profiles of vibrational temperature and species number density generated by the conventional MT approach are compared with that of the STS approach. Modification of the governing parameters, namely, dissociation RC and C_{DV}, is proposed to improve the accuracy of the MT method. Specifically, it is recommended to use the QSS dissociation RC rather than the equilibrium RC and the temperature-dependent approximation of C_{DV} to avoid serious discrepancies between MT and STS approaches at high temperatures.

The O_2–N_2 vibrational relaxation time and dissociation RC based on QCT simulations are given for the first time in the literature using a high-fidelity ab-initio six-dimensional PES. The present QCT data are in very good agreement with the experimental measurements by

General and Losev [74]. At the same time, the difficulties and inaccuracies of the QCT approach are recognized when attempting to generate state-specific rates for temperatures below 4000 K. This can be attributed to the failure of the QCT method to describe quantum effects at low temperatures and for low-lying vibrational states. At these temperatures, the QCT method strongly underestimates the true RCs, which can obtained by a more rigorous approach at higher computational cost. Because these temperatures are still of interest for hypersonic simulations, one can recommend the combination of semi- and quasi-classical trajectory approaches to access the wide range of collisional energies.

Acknowledgment

References

[1] Schinke, R., Grebenshchikov, S. Y., Ivanov, M., and Fleurat-Lessard, P., "Dynamical Studies of the Ozone Isotope Effect: A Status Report," *Annual Review of Physical Chemistry*, Vol. 57, No. 1, 2006, pp. 625–661.
doi:10.1146/annurev.physchem.57.032905.104542

[2] Aquilanti, V., Bartolomei, M., Carmona-Novillo, E., and Pirani, F., "The Asymmetric Dimer N_2–O_2: Characterization of the Potential Energy Surface and Quantum Mechanical Calculation of Rotovibrational Levels," *Journal of Chemical Physics*, Vol. 118, No. 5, 2003, pp. 2214–2222.
doi:10.1063/1.1533015

[3] Varandas, A., and Pais, A., "Double Many-Body Expansion Potential Energy Surface for $O_4(^3A)$, Dynamics of the $O(^3P) + O_3(^1A_1)$ Reaction, and Second Virial Coefficients of Molecular Oxygen," *Theoretical and Computational Models for Organic Chemistry*, Springer–Verlag, New York, 1991, pp. 55–78.

[4] Bender, J. D., Valentini, P., Nompelis, I., Schwartzentruber, T., and Candler, G. V., "Characterization of Vibrational and Rotational Energy Transfer in $N_2 + N_2$ Dissociative Collisions Using the Quasiclassical Trajectory Method," *45th AIAA Thermophysics Conference*, AIAA Paper 2015-3253, June 2015.

[5] Bender, J. D., Valentini, P., Nompelis, I., Paukku, Y., Varga, Z., Truhlar, D. G., Schwartzentruber, T., and Candler, G. V., "An Improved Potential Energy Surface and Multi-Temperature Quasiclassical Trajectory Calculations of $N_2 + N_2$ Dissociation Reactions," *Journal of Chemical Physics*, Vol. 143, No. 5, 2015, Paper 054304.
doi:10.1063/1.4927571

[6] Panesi, M., Jaffe, R. L., Schwenke, D. W., and Magin, T. E., "Rovibrational Internal Energy Transfer and Dissociation of $N_2(^1\Sigma_g^+)$–$N(^4S_u)$ System in Hypersonic Flows," *Journal of Chemical Physics*, Vol. 138, No. 4, 2013, Paper 044312.
doi:10.1063/1.4774412

[7] Panesi, M., Munafo, A., Magin, T., and Jaffe, R., "Nonequilibrium Shock-Heated Nitrogen Flows Using a Rovibrational State-to-State Method," *Physical Review E: Statistical, Nonlinear, and Soft Matter Physics*, Vol. 90, No. 1, 2014, Paper 013009.
doi:10.1103/PhysRevE.90.013009

[8] Bruno, D., Capitelli, M., Esposito, F., Longo, S., and Minelli, P., "Direct Simulation of Non-Equilibrium Kinetics Under Shock Conditions in Nitrogen," *Chemical Physics Letters*, Vol. 360, No. 1, 2002, pp. 31–37.
doi:10.1016/S0009-2614(02)00772-8

[9] Esposito, F., Capitelli, M., and Gorse, C., "Quasi-Classical Dynamics and Vibrational Kinetics of $N + N_2(v)$ System," *Chemical Physics*, Vol. 257, Nos. 2–3, 2000, pp. 193–202.

[10] Esposito, F., and Capitelli, M., "QCT Calculations for the Process $N_2(v) + N \rightarrow N_2(v') + N$ in the Whole Vibrational Range," *Chemical Physics Letters*, Vol. 418, No. 4, 2006, pp. 581–585.
doi:10.1016/j.cplett.2005.11.036

[11] Kim, J. G., and Boyd, I. D., "State-Resolved Master Equation Analysis of Thermochemical Nonequilibrium of Nitrogen," *Chemical Physics*, Vol. 415, March 2013, pp. 237–246.
doi:10.1016/j.chemphys.2013.01.027

[12] Bose, D., and Candler, G. V., "Thermal Rate Constants of the $N_2 + O \rightarrow NO + N$ Reaction Using Abinitio $3A''$ and $3A'$ Potential Energy Surfaces," *Journal of Chemical Physics*, Vol. 104, No. 8, 1996,

pp. 2825–2833.
doi:10.1063/1.471106

[13] McClinton, C. R., "X-43 Scramjet Power Breaks the Hypersonic Barrier: Dryden Lectureship in Research for 2006," *44th AIAA Aerospace Sciences Meeting and Exhibit*, AIAA Paper 2006-1, Jan. 2006.

[14] Yamashita, K., Morokuma, K., Le Quéré, F., and Leforestier, C., "New Ab Initio Potential Surfaces and Three-Dimensional Quantum Dynamics for Transition State Spectroscopy in Ozone Photo-dissociation," *Chemical Physics Letters*, Vol. 191, No. 6, 1992, pp. 515–520.
doi:10.1016/0009-2614(92)85582-U

[15] Siebert, R., Fleurat-Lessard, P., Schinke, R., Bittererová, M., and Farantos, S., "The Vibrational Energies of Ozone up to the Dissociation Threshold: Dynamics Calculations on an Accurate Potential Energy Surface," *Journal of Chemical Physics*, Vol. 116, No. 22, 2002, p. 9749.
doi:10.1063/1.1473664

[16] Tyuterev, V. G., Tashkun, S., Jensen, P., Barbe, A., and Cours, T., "Determination of the Effective Ground State Potential Energy Function of Ozone from High-Resolution Infrared Spectra," *Journal of Molecular Spectroscopy*, Vol. 198, No. 1, 1999, pp. 57–76.
doi:10.1006/jmsp.1999.7928

[17] Varandas, A., and Pais, A., "A Realistic Double Many-Body Expansion (DMBE) Potential Energy Surface for Ground-State O_3 from a Multiproperty Fit to Ab Initio Calculations, and to Experimental Spectroscopic, Inelastic Scattering, and Kinetic Isotope Thermal Rate Data," *Molecular Physics*, Vol. 65, No. 4, Nov. 1988, pp. 843–860.
doi:10.1080/00268978800101451

[18] Webster, H., III, and Bair, E. J., "Ozone Ultraviolet Photolysis. IV. $O_2 + O(^3P)$ Vibrational Energy Transfer," *Journal of Chemical Physics*, Vol. 56, No. 12, 1972, pp. 6104–6108.
doi:10.1063/1.1677161

[19] Andrienko, D., and Boyd, I. D., "Investigation of Oxygen Vibrational Relaxation by Quasi-Classical Trajectory Method," *Chemical Physics*, Vol. 459, Sept. 2015, pp. 1–0.
doi:10.1016/j.chemphys.2015.07.023

[20] Andrienko, D. A., and Boyd, I. D., "Rovibrational Energy Transfer and Dissociation in O_2–O Collisions," *Journal of Chemical Physics*, Vol. 144, No. 10, 2016, Paper 104301.
doi:10.1063/1.4943114

[21] Esposito, F., and Capitelli, M., "The Relaxation of Vibrationally Excited O_2 Molecules by Atomic Oxygen," *Chemical Physics Letters*, Vol. 443, No. 4, 2007, pp. 222–226.
doi:10.1016/j.cplett.2007.06.099

[22] Esposito, F., Armenise, I., Capitta, G., and Capitelli, M., "$O + O_2$ State-to-State Vibrational Relaxation and Dissociation Rates Based on Quasiclassical Calculations," *Chemical Physics*, Vol. 351, Nos. 1–3, 2008, pp. 91–98.
doi:10.1016/j.chemphys.2008.04.004

[23] Kulakhmetov, M., Gallis, M., and Alexeenko, A., "Effect of $O_2 + O$ Ab Initio and Morse Additive Pairwise Potentials on Dissociation and Relaxation Rates for Nonequilibrium Flow Calculations," *Physics of Fluids*, Vol. 27, No. 8, 2015, Paper 087104.
doi:10.1063/1.4928198

[24] Coletti, C., and Billing, G. D., "Vibrational Energy Transfer in Molecular Oxygen Collisions," *Chemical Physics Letters*, Vol. 356, No. 1, 2002, pp. 14–22.
doi:10.1016/S0009-2614(02)00279-8

[25] Billing, G. D., and Kolesnick, R., "Vibrational Relaxation of Oxygen. State to State Rate Constants," *Chemical Physics Letters*, Vol. 200, No. 4, 1992, pp. 382–386.
doi:10.1016/0009-2614(92)87008-D

[26] Billing, G. D., "VV and VT Rates in N_2–O_2 Collisions," *Chemical Physics*, Vol. 179, No. 3, 1994, pp. 463–467.
doi:10.1016/0301-0104(94)87022-5

[27] Park, H., and Slanger, T., "$O_2(X, v = 8$–$22)$ 300 K Quenching Rate Coefficients for O_2 and N_2, and $O_2(X)$ Vibrational Distribution from 248 nm O_3 Photodissociation," *Journal of Chemical Physics*, Vol. 100, No. 1, 1994, pp. 287–300.
doi:10.1063/1.466997

[28] Price, J., Mack, J., Rogaski, C., and Wodtke, A., "Vibrational-State-Specific Self-Relaxation Rate Constant. Measurements of Highly Vibrationally Excited $O_2(v = 19$–$28)$," *Chemical Physics*, Vol. 175, No. 1, 1993, pp. 83–98.
doi:10.1016/0301-0104(93)80230-7

[29] Varandas, A., "Are Vibrationally Excited Molecules a Clue for the O_3 Deficit Problem and HO_x Dilemma in the Middle Atmosphere?" *Journal of Physical Chemistry A*, Vol. 108, No. 5, 2004, pp. 758–769.
doi:10.1021/jp036321p

[30] Bender, J., Nompelis, I., Valentini, P., Schwartzentruber, T., Candler, G. V., Doraiswamy, S., Paukku, Y. K., Yang, K. R., Varga, Z., and Truhlar, D. G., "Quasiclassical Trajectory Analysis of the $N_2 + N_2$ Reaction Using a New Ab Initio Potential Energy Surface," *11th AIAA/ASME Joint Thermophysics and Heat Transfer Conference*, AIAA Paper 2014-2964, June 2014.

[31] Varga, Z., Meana-Pañeda, R., Song, G., Paukku, Y., and Truhlar, D. G., "Potential Energy Surface of Triplet N_2O_2," *Journal of Chemical Physics*, Vol. 144, No. 2, 2016, Paper 024310.
doi:10.1063/1.4939008

[32] Jaffe, R., Schwenke, D., and Chaban, G., "Vibrational and Rotational Excitation and Dissociation in N_2–N_2 Collisions from Accurate Theoretical Calculations," *10th AIAA/ASME Joint Thermophysics and Heat Transfer Conference*, AIAA Paper 2010-4517, June 2010.

[33] Paukku, Y., Yang, K. R., Varga, Z., and Truhlar, D. G., "Global Ab Initio Ground-State Potential Energy Surface of N_4," *Journal of Chemical Physics*, Vol. 139, No. 4, 2013, Paper 044309.
doi:10.1063/1.4811653

[34] Koura, K., "Monte Carlo Direct Simulation of Rotational Relaxation of Diatomic Molecules Using Classical Trajectory Calculations: Nitrogen Shock Wave," *Physics of Fluids*, Vol. 9, No. 11, 1997, pp. 3543–3549.
doi:10.1063/1.869462

[35] Secrest, D., and Johnson, B. R., "Exact Quantum-Mechanical Calculation of a Collinear Collision of a Particle with a Harmonic Oscillator," *Journal of Chemical Physics*, Vol. 45, No. 12, 1966, pp. 4556–4570.
doi:10.1063/1.1727537

[36] Light, J. C., "Quantum Calculations in Chemically Reactive Systems," *Methods of Computational Physics*, Vol. 10, Academic Press, New York, 2012, pp. 111–142.

[37] Meyer, H.-D., Manthe, U., and Cederbaum, L. S., "The Multi-Configurational Time-Dependent Hartree Approach," *Chemical Physics Letters*, Vol. 165, No. 1, 1990, pp. 73–78.
doi:10.1016/0009-2614(90)87014-I

[38] Billing, G. D., "Semiclassical Theory for Diatom-Diatom Collisions," *Chemical Physics Letters*, Vol. 97, No. 2, 1983, pp. 188–192.
doi:10.1016/0009-2614(83)85014-3

[39] Cacciatore, M., Kurnosov, A., and Napartovich, A., "Vibrational Energy Transfer in N_2–N_2 Collisions: A New Semiclassical Study," *Journal of Chemical Physics*, Vol. 123, No. 17, 2005, Paper 174315.
doi:10.1063/1.2101445

[40] Miller, W. H., "Semiclassical Nature of Atomic and Molecular Collisions," *Accounts of Chemical Research*, Vol. 4, No. 5, 1971, pp. 161–167.
doi:10.1021/ar50041a001

[41] Heller, E. J., "Time-Dependent Approach to Semiclassical Dynamics," *Journal of Chemical Physics*, Vol. 62, No. 4, 1975, pp. 1544–1555.
doi:10.1063/1.430620

[42] Truhlar, D. G., and Muckerman, J. T., "Reactive Scattering Cross Sections III: Quasiclassical and Semiclassical Methods," *Atom-Molecule Collision Theory*, Springer–Verlag, New York, 1979, pp. 505–566.

[43] Miller, W. H., "Classical-Limit Quantum Mechanics and the Theory of Molecular Collisions," *Advances in Chemical Physics*, Vol. 25, No. 1, 1974, pp. 69–177.

[44] Ulusoy, I., Andrienko, D., Boyd, I., and Hernandez, R., "Quantum and Quasi-Classical Collisional Dynamics of O_2–Ar at High Temperatures," *Journal of Chemical Physics*, Vol. 144, No. 23, 2016, Paper 234311.
doi:10.1063/1.4954041

[45] Garcia, E., Kurnosov, A., Lagana, A., Pirani, F., Bartolomei, M., and Cacciatore, M., "Efficiency of Collisional $O_2 + N_2$ Vibrational Energy Exchange," *Journal of Physical Chemistry B*, Vol. 120, No. 8, 2015, pp. 1476–1485.

[46] Kim, J. G., and Boyd, I. D., "Thermochemical Nonequilibrium Modeling of Electronically Excited Molecular Oxygen," *11th AIAA/ASME Joint Thermophysics and Heat Transfer Conference*, AIAA Paper 2014-2963, June 2014.

[47] Andrienko, D., and Boyd, I. D., "Thermal Relaxation of Molecular Oxygen in Collisions with Nitrogen Atoms," *Journal of Chemical Physics*, Vol. 145, No. 1, 2016, Paper 014309.
doi:10.1063/1.4955199

[48] Sayós, R., Oliva, C., and Gonzalez, M., "New Analytical ($2A'$, $4A'$) Surfaces and Theoretical Rate Constants for the $N(^4S) + O_2$ Reaction," *Journal of Chemical Physics*, Vol. 117, No. 2, 2002, pp. 670–679.
doi:10.1063/1.1483853

[49] Raff, L. M., Thompson, D. L., Sims, L., and Porter, R. N., "Dynamics of the Molecular and Atomic Mechanisms for the Hydrogen-Iodine Exchange Reaction," *Journal of Chemical Physics*, Vol. 56, No. 12,

1972, pp. 5998–6027.
doi:10.1063/1.1677149

[50] Panesi, M., and Lani, A., "Collisional Radiative Coarse-Grain Model for Ionization in Air," *Physics of Fluids*, Vol. 25, No. 5, 2013, Paper 057101.
doi:10.1063/1.4804388

[51] Park, C., *Nonequilibrium Hypersonic Aerothermodynamics*, Wiley, New York, 1989.

[52] Park, C., "Rotational Relaxation of N_2 Behind a Strong Shock Wave," *Journal of Thermophysics and Heat Transfer*, Vol. 18, No. 4, 2004, pp. 527–533.
doi:10.2514/1.11442

[53] Shatalov, O., "Molecular Dissociation of Oxygen in the Absence of Vibrational Equilibrium," *Combustion, Explosion, and Shock Waves*, Vol. 9, No. 5, 1973, pp. 610–613.
doi:10.1007/BF00742888

[54] Kalogerakis, K. S., Copeland, R. A., and Slanger, T. G., "Measurement of the Rate Coefficient for Collisional Removal of $O_2(X^3\Sigma_g^-, v = 1)$ by $O(^3P)$," *Journal of Chemical Physics*, Vol. 123, No. 19, 2005, Paper 194303.
doi:10.1063/1.2110227

[55] Pejaković, D. A., Campbell, Z., Kalogerakis, K. S., Copeland, R. A., and Slanger, T. G., "Collisional Relaxation of $O_2(X^3\sum_g^-, v = 1)$ and $(a^1\Delta_g, v = 1)$ by Atmospherically Relevant Species," *Journal of Chemical Physics*, Vol. 135, No. 9, 2011, Paper 094309.

[56] Breen, J., Quy, R., and Glass, G., "Vibrational Relaxation of O_2 in the Presence of Atomic Oxygen," *Journal of Chemical Physics*, Vol. 59, No. 1, 1973, pp. 556–557.
doi:10.1063/1.1679846

[57] Kiefer, J. H., and Lutz, R. W., "The Effect of Oxygen Atoms on the Vibrational Relaxation of Oxygen," *Symposium (International) on Combustion*, Vol. 11, Elsevier, New York, 1967, pp. 67–76.

[58] Millikan, R. C., and White, D. R., "Systematics of Vibrational Relaxation," *Journal of Chemical Physics*, Vol. 39, No. 12, 1963, pp. 3209–3213.
doi:10.1063/1.1734182

[59] Park, C., "Review of Chemical-Kinetic Problems of Future NASA Missions. I—Earth Entries," *Journal of Thermophysics and Heat Transfer*, Vol. 7, No. 3, 1993, pp. 385–398.
doi:10.2514/3.431

[60] Capitelli, M., Ferreira, C. M., Osipov, A. I., and Gordiets, B. F., *Plasma Kinetics in Atmospheric Gases*, Springer–Verlag, New York, 2000.

[61] Neitzel, K., Andrienko, D., and Boyd, I. D., "Modeling Fidelity for Oxygen Nonequilibrium Thermochemistry in Reflected Shock Tube Flows," *45th AIAA Thermophysics Conference*, AIAA Paper 2015-2509, June 2015.

[62] Ibraguimova, L., Sergievskaya, A., Levashov, V. Y., Shatalov, O., Tunik, Y. V., and Zabelinskii, I., "Investigation of Oxygen Dissociation and Vibrational Relaxation at Temperatures 4000–10,800 k," *Journal of Chemical Physics*, Vol. 139, No. 3, 2013, Paper 034317.
doi:10.1063/1.4813070

[63] Bykova, N., and Kuznetsova, L., "Study of the Absorption Characteristics of Molecular Oxygen in the Schumann-Runge System at High Temperatures: I. Calculations of Absorption Spectra," *Optics and Spectroscopy*, Vol. 105, No. 5, 2008, pp. 668–673.
doi:10.1134/S0030400X08110040

[64] Andrienko, D. A., and Boyd, I. D., "High Fidelity Modeling of Thermal Relaxation and Dissociation of Oxygen," *Physics of Fluids*, Vol. 27, No. 11, 2015, Paper 116101.
doi:10.1063/1.4935241

[65] Park, C., "Thermochemical Relaxation in Shock Tunnels," *Journal of Thermophysics and Heat Transfer*, Vol. 20, No. 4, 2006, pp. 689–698.
doi:10.2514/1.22719

[66] Eckstrom, D., "Vibrational Relaxation of Shock-Heated N_2 by Atomic Oxygen Using the IR Tracer Method," *Journal of Chemical Physics*, Vol. 59, No. 6, 1973, pp. 2787–2795.
doi:10.1063/1.1680410

[67] McNeal, R. J., Whitson, M. E., and Cook, G. R., "Temperature Dependence of the Quenching of Vibrationally Excited Nitrogen by Atomic Oxygen," *Journal of Geophysical Research*, Vol. 79, No. 10, 1974, pp. 1527–1531.
doi:10.1029/JA079i010p01527

[68] Breshears, W., and Bird, P., "Effect of Oxygen Atoms on the Vibrational Relaxation of Nitrogen," *Journal of Chemical Physics*, Vol. 48, No. 10, 1968, pp. 4768–4773.
doi:10.1063/1.1668060

[69] Valentini, P., Schwartzentruber, T. E., Nompelis, I., and Candler, G. V., "Ab Initio Based Model for High Temperature Nitrogen Rovibrational

Excitation and Dissociation," *54th AIAA SCITECH Conference*, AIAA Paper 2016-0500, Jan. 2016.

[70] Bartolomei, M., Carmona-Novillo, E., Hernández, M. I., Campos-Martnez, J., and Moszynski, R., "Global Ab Initio Potential Energy Surface for the $O_2(^3\Sigma_g^-) + N_2(^1\Sigma_g^+)$ Interaction. Applications to the Collisional, Spectroscopic, and Thermodynamic Properties of the Complex," *Journal of Physical Chemistry A*, Vol. 118, No. 33, 2014, pp. 6584–6594.
doi:10.1021/jp503182h

[71] Gilmore, F. R., Bauer, E., and McGowan, J. W., "A Review of Atomic and Molecular Excitation Mechanisms in Nonequilibrium Gases up to 20,000°K," *Journal of Quantitative Spectroscopy and Radiative Transfer*, Vol. 9, No. 2, 1969, pp. 157–183.
doi:10.1016/0022-4073(69)90084-3

[72] White, D., "Shock-Tube Study of Vibrational Exchange in N_2–O_2 Mixtures," *Journal of Chemical Physics*, Vol. 49, No. 12, 1968, pp. 5472–5476.
doi:10.1063/1.1670074

[73] White, D. R., and Millikan, R. C., "Vibrational Relaxation in Air," *AIAA Journal*, Vol. 2, No. 10, 1964, pp. 1844–1846.
doi:10.2514/3.2687

[74] Generalov, N., and Losev, S., "Vibrational Excitation and Decomposition of Molecular Oxygen and Carbon Dioxide Behind Shock Waves," *Journal of Quantum Spectroscopy and Radiative Transfer*, Vol. 6, No. 1, 1966, pp. 101–125.
doi:10.1016/0022-4073(66)90066-5

[75] Wray, K. L., "Chemical Kinetics of High Temperature Air," Avco-Everett Research Lab., Avco Corp., Everett, MA, 1961.

[76] Jerig, L., Thielen, K., and Roth, P., "High-Temperature Dissociation of Oxygen Diluted in Argon or Nitrogen," *AIAA Journal*, Vol. 29, No. 7, 1991, pp. 1136–1139.
doi:10.2514/3.10714

This article has been cited by:

1. Kenji Miki. Uncertainty Quantification on the High-Temperature Kinetics of Dioxygen Dissociation and Oxygen Recombination. *Journal of Thermophysics and Heat Transfer*, ahead of print1-11. [Abstract] [Full Text] [PDF] [PDF Plus]

2. Daniil Andrienko, Iain D. Boyd. Master equation simulation of O2-N2 collisions on an ab-initio potential energy surface . [Citation] [PDF] [PDF Plus]